

# Synthesis of Nonfluorinated Amphiphilic Rod–Coil Block Copolymer and Its Application to Proton Exchange Membrane

Tae Ann Kim and Won Ho Jo\*

WCU Hybrid Materials Program, Department of Materials Science and Engineering,  
Seoul National University, Seoul 151-742, Korea

Received March 2, 2010. Revised Manuscript Received May 10, 2010

New amphiphilic block copolymers composed of thermally and chemically stable poly(arylene sulfone ether ketone) and sulfonated poly(styrene-*co*-acrylonitrile) were successfully synthesized through two-step polymerization, condensation polymerization followed by controlled radical polymerization, for application to proton exchange membrane fuel cells. The morphological structures of membranes were investigated as functions of the hydrophilic chain length and the degree of sulfonation (DS), and were related to the proton conductivity of the membranes. Because of their inherent high thermal stability and well-connected hydrophilic channel, the newly synthesized membranes show high proton conductivity at relatively low DS and a continuous increase in proton conductivity above 90 °C. They also exhibit good thermal and oxidative stability.

## Introduction

A proton exchange membrane (PEM) is the most essential component of proton exchange membrane fuel cell (PEMFC).<sup>1–3</sup> A critical requirement for high-efficiency PEM is sufficient proton conductivity. Generally, PEMs are composed of hydrophobic and hydrophilic segments in one macromolecule, which can generate hydrophobic/hydrophilic nanophase separation. In the presence of water, a hydrophilic domain formed by aggregation of acid functional groups is hydrated and proton charge carriers are transferred through this domain.<sup>4</sup> Therefore, a well-connected hydrophilic channel is extremely important to obtain high-performance PEMs. For the specific case of Dupont's Nafion, which exhibits high proton conductivity, the hydrophilic domains in the fully hydrated film form an interconnecting proton conductive network with a characteristic dimension of 5 nm.<sup>5</sup>

Another important requirement for high-performance PEM is an increase in the operating temperature. The operation at high temperatures above 100 °C has numerous benefits: (i) improved tolerance of Pt catalyst to contaminants, (ii) accelerated reaction kinetics at both electrodes, (iii) facilitation of water management, and (iv)

alleviation of the cooling system.<sup>6–8</sup> However, at high temperatures, the conductivity of perfluorosulfonic acid polymers such as Nafion decreases drastically due to the loss of water; this change in conductivity is accompanied by considerable deterioration in the mechanical strength of the membranes. To overcome these problems, much effort has been made on development of new proton exchange membranes including modified perfluorosulfonic acid polymers,<sup>9–11</sup> sulfonated aromatic hydrocarbon polymers,<sup>12–14</sup> and acid–base polymer membranes.<sup>15,16</sup>

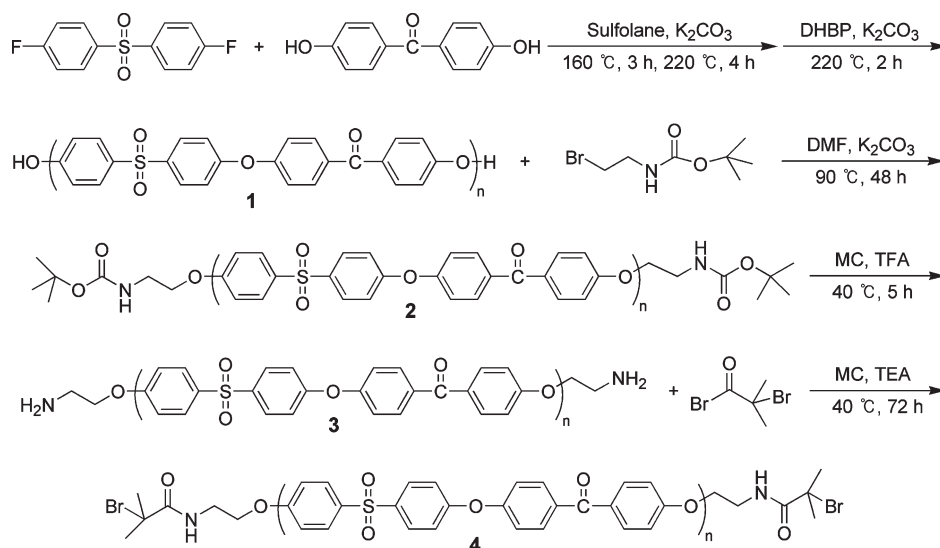
High-performance aromatic polymers are excellent alternatives to Nafion membrane, because high-performance polymers, such as poly(arylene ether sulfone)s, poly(aryl ether ketone)s, and poly(phenylene oxide)s, possess excellent thermal and mechanical stability, and good oxidative resistance; moreover, their production cost is much lower than that of Nafion. Among these polymers, poly(arylene ether sulfone)s<sup>17,18</sup> and poly(arylene ether ketone)s,<sup>19</sup> both of which contain sulfonate groups, have been extensively

\*Corresponding author. Tel.: +82 2 880 7192; fax: +82 2 876 6086; e-mail: whjpoly@snu.ac.kr.

- (1) Rikukawa, M.; Sanui, K. *Prog. Polym. Sci.* **2000**, *25*, 1463.
- (2) Steele, B. C. H.; Heinzl, A. *Nature* **2001**, *414*, 345.
- (3) Hickner, M. A.; Ghassemi, H.; Kim, Y. S.; Einsla, B. R.; McGrath, J. E. *Chem. Rev.* **2004**, *104*, 4587.
- (4) Kreuer, K. D. *J. Membr. Sci.* **2001**, *185*, 29.
- (5) Lin, J.; Wu, P. H.; Wycisk, R.; Pintauro, P. N.; Shi, Z. Q. *Macromolecules* **2008**, *41*, 4284.
- (6) Zhang, J. L.; Xie, Z.; Zhang, J. J.; Tanga, Y. H.; Song, C. J.; Navessin, T.; Shi, Z. Q.; Song, D. T.; Wang, H. J.; Wilkinson, D. P.; Liu, Z. S.; Holdcroft, S. *J. Power Sources* **2006**, *160*, 872.
- (7) Athens, G. L.; Ein-Eli, Y.; Chmelka, B. F. *Adv. Mater.* **2007**, *19*, 2580.

- (8) Shao, Y. Y.; Yin, G. P.; Wang, Z. B.; Gao, Y. Z. *J. Power Sources* **2007**, *167*, 235.
- (9) Wang, H. T.; Holmberg, B. A.; Huang, L. M.; Wang, Z. B.; Mitra, A.; Norbeck, J. M.; Yan, Y. S. *J. Mater. Chem.* **2002**, *12*, 834.
- (10) Chen, W. F.; Kuo, P. L. *Macromolecules* **2007**, *40*, 1987.
- (11) Pereira, F.; Valle, K.; Belleville, P.; Morin, A.; Lambert, S.; Sanchez, C. *Chem. Mater.* **2008**, *20*, 1710.
- (12) Wang, F.; Hickner, M.; Ji, Q.; Harrison, W.; Mecham, J.; Zawodzinski, T. A.; McGrath, J. E. *Macromol. Symp.* **2001**, *175*, 387.
- (13) Asano, N.; Aoki, M.; Suzuki, S.; Miyatake, K.; Uchida, H.; Watanabe, M. *J. Am. Chem. Soc.* **2006**, *128*, 1762.
- (14) Matsumoto, K.; Higashihara, T.; Ueda, M. *Macromolecules* **2008**, *41*, 7560.
- (15) Schechter, A.; Savinell, R. F. *Solid State Ionics* **2002**, *147*, 181.
- (16) Weber, J.; Kreuer, K. D.; Maier, J.; Thomas, A. *Adv. Mater.* **2008**, *20*, 2595.
- (17) Harrison, W. L.; Hickner, M. A.; Kim, Y. S.; McGrath, J. E. *Fuel Cells* **2005**, *5*, 201.
- (18) Roy, A.; Lee, H. S.; McGrath, J. E. *Polymer* **2008**, *49*, 5037.
- (19) Zhao, C. J.; Lin, H. D.; Shao, K.; Li, X. F.; Ni, H. Z.; Wang, Z.; Na, H. *J. Power Sources* **2006**, *162*, 1003.

Scheme 1. Synthetic Scheme of PSEK Macroinitiator



investigated to determine their suitability to high-temperature fuel cell applications. However, to achieve high proton conductivity that is comparable to that of Nafion, a high degree of sulfonation is required, which in turn leads to a decrease in electrochemical and dimensional stability.

In this study, we synthesized a novel rod-coil block copolymer comprising poly(arylene sulfone ether ketone) (PSEK) and sulfonated poly(styrene-*co*-acrylonitrile) (PSAN) for PEM. We were motivated to design this unique polymer for the following reasons. First, well-defined hydrophilic and hydrophobic phase morphologies can be formed in block copolymers.<sup>20–24</sup> Second, the coil block (sulfonated PSAN block), which has higher flexibility than aromatic polymers, can easily develop phase separation and form a well-ordered ion channel. Third, both blocks of the block copolymer are thermally and chemically stable, which enable high-temperature operation. Herein, we report on the synthesis of the new rod-coil block copolymer, and the effects of hydrophilic chain length and the degree of sulfonation on the morphology, proton conductivity, and thermal and chemical stability of the newly developed block copolymer are systematically analyzed.

## Results and Discussion

**Synthesis and Characterization of Rod-Coil Block Copolymers.** PSEK macroinitiator (**4** in Scheme 1) was synthesized through polycondensation of 4,4'-difluorodiphenyl sulfone (DFDPS) with 4,4'-dihydroxy benzophenone (DHBP) followed by the end group modification, as shown in Scheme 1. To synthesize hydroxyl terminated

PSEK (**1**), an excess of DHBP was used. The number-average molecular weight and the polydispersity index of **1**, as determined by gel permeation chromatography (GPC), are 18 kg/mol and 1.52, respectively. Hydroxyl end groups of **1** were first converted to amine terminated PSEK (**3**) through two-step reactions, and then the amine end groups were reacted with  $\alpha$ -bromoisobutyryl bromide to produce an ATRP macroinitiator (**4**). It is noteworthy that the chain ends of the macroinitiator contain an amide linkage which is more resistant in an acidic environment than an ester linkage. Since all <sup>1</sup>H NMR signals of **4** were properly assigned, as shown in Figure 1a, the chemical structure of **4** was successfully identified. FT-IR spectra of the resulting polymers also provided further evidence for the complete end group modification (See Supporting Information, Figure S1).

The PSEK macroinitiator was extended with a mixture of an azeotropic feed composition of styrene (St) and acrylonitrile (AN) (ca. 60 mol % styrene) using an activator regenerated by the electron transfer atom transfer radical polymerization (ARGET ATRP) (Scheme 2). It should be noted here that the recently introduced ARGET ATRP allows us to polymerize at considerably low catalyst concentration, because of the continuous regeneration of the catalyst by various reducing agents.<sup>25</sup> The low catalyst concentration also contributes to considerable suppression of side reactions originating from outer-sphere electron transfer reactions with the catalyst; this permits the formation of high-molecular-weight PSAN with low polydispersity.<sup>26,27</sup>

Three block copolymers with different block lengths of PSAN were synthesized by controlling the reaction time. The chemical structure of PSEK-*b*-PSAN (**5**) was identified by <sup>1</sup>H NMR (Figure 1b), and the molecular weights and the polydispersity indices of **5** were in the range of 49–110 kg/mol and 1.52–1.86, respectively, as determined by GPC (Table 1).

- (20) Shin, C. K.; Maier, G.; Andreaus, B.; Scherer, G. G. *J. Membr. Sci.* **2004**, *245*, 147.  
 (21) Park, M. J.; Downing, K. H.; Jackson, A.; Gomez, E. D.; Minor, A. M.; Cookson, D.; Weber, A. Z.; Balsara, N. P. *Nano Lett.* **2007**, *7*, 3547.  
 (22) Schonberger, F.; Kerres, J. J. *Polym. Sci., Polym. Chem.* **2007**, *45*, 5237.  
 (23) Roy, A.; Yu, X.; Dunn, S.; McGrath, J. E. *J. Membr. Sci.* **2009**, *327*, 118.  
 (24) Choi, W. H.; Jo, W. H. *J. Power Sources* **2009**, *188*, 127.

- (25) Jakubowski, W.; Min, K.; Matyjaszewski, K. *Macromolecules* **2006**, *39*, 39.  
 (26) Pietrasik, J.; Dong, H. C.; Matyjaszewski, K. *Macromolecules* **2006**, *39*, 6384.  
 (27) Tsarevsky, N. V.; Sarbu, T.; Gobelt, B.; Matyjaszewski, K. *Macromolecules* **2002**, *35*, 6142.

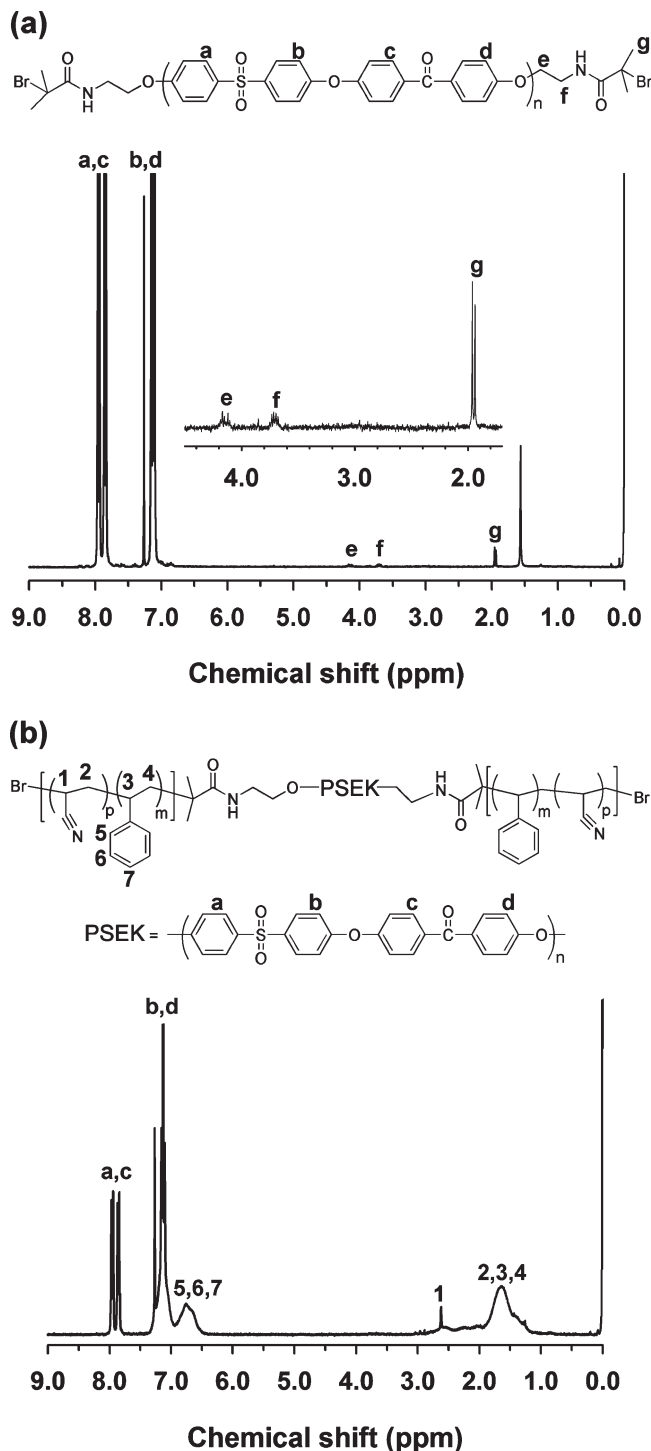


**Figure 1.** <sup>1</sup>H NMR spectra of (a) PSEK macroinitiator, and (b) PSEK-*b*-PSAN in CDCl<sub>3</sub>.

Since the GPC trace of **5** exhibits monomodality (Figure 2), it is obvious that the block copolymer does not contain unreacted PSEK macroinitiator.

Sulfonation of the block copolymers was carried out with acetyl sulfate (Scheme 2). It has been reported that the sulfonation of styrene-containing polymers with acetyl

sulfate results in selective sulfonation at the *para*-position of the aromatic ring in styrene unit.<sup>28,29</sup> Indeed, when PSEK was treated with acetyl sulfate under the identical condition of sulfonation, PSEK was not sulfonated. Nine samples with different degrees of sulfonation (DS) were prepared by changing the amount of sulfonation reagent, as listed in Table 2. Sulfonation of block copolymers was confirmed by FT-IR spectroscopy. When FT-IR spectra of the block copolymer before and after sulfonation are compared, as shown in Figure 3, the spectrum of the block copolymer after sulfonation shows three characteristic peaks at 1380, 1035, and 1008 cm<sup>-1</sup>, which correspond to S=O antisymmetric stretching of sulfonic acid, symmetric stretching of the sulfonate group, and in-plane bending of the *para*-substituted phenyl ring of polystyrene, respectively, whereas the spectrum before sulfonation does not exhibit such peaks. When the DS was determined from elemental analysis, the maximum DS was 9.3%. An attempt to increase the DS by adding an excess amount of acetyl sulfate was not successful, because of poor solubility of acetyl sulfate in such reaction system.<sup>30</sup>

**Morphology.** To induce microphase separation of block copolymers without possible degradation due to the presence of sulfonic acid groups at high temperature, all membranes were solvent-annealed: they were placed in saturated dimethylacetamide vapor at 50 °C for 24 h. Figure 4 shows a set of morphological images of membranes with different lengths of hydrophilic block (sulfonated PSAN block). As the block length of hydrophilic block (the coil part in the rod-coil block copolymer) increases, the morphology changes from hexagonally packed cylinder (HEX) structure [**6**(18/12-7)], hexagonally perforated lamellar (HPL) structure [**6**(18/27-9)] to well-ordered lamellar (LAM) structure [**6**(18/42-9)]. The self-assembly of rod-coil block copolymers is fundamentally different from that of coil-coil block copolymers, because rod-shaped chains exhibit different scaling behavior from coil-shaped ones as a function of molecular weight. This difference in scaling creates a mismatch in size that is not captured by the coil fraction and requires the additional parameter that is related to the ratio of the rod and coil block lengths.<sup>31,32</sup> Therefore, the block copolymer **6**(18/42-9) can form lamellar structure, although it has large molecular weight difference between two blocks.

When the effect of DS on the lamellar spacing is examined, it is observed that the lamellar spacing increases with increasing the DS, as shown in Figure 5: The interlamellar spacings of **6**(18/42-2), **6**(18/42-6), and **6**(18/42-9), as estimated from Figure 5, are 56.7 nm, 62.9 nm, and 65.7 nm, respectively. The increase of lamellar spacing with DS is due to an increase in the volume fraction of hydrophilic block with the introduction of bulky sulfonic acid groups.

**Proton Conductivity.** When the proton conductivity of membranes with different hydrophilic chain length

(28) Smitha, B.; Sridhar, S.; Khan, A. A. *J. Membr. Sci.* **2003**, 225, 63.

(29) Norsten, T. B.; Guiver, M. D.; Murphy, J.; Astill, T.; Navessin, T.; Holderoft, S.; Frankamp, B. L.; Rotello, V. M.; Ding, J. F. *Adv. Funct. Mater.* **2006**, 16, 1814.

(30) Zhang, X. P.; Liu, S. Z.; Yin, J. J. *J. Membr. Sci.* **2005**, 258, 78.

(31) Lee, M.; Cho, B. K.; Zin, W. C. *Chem. Rev.* **2001**, 101, 3869.

(32) Olsen, B. D.; Segalman, R. A. *Mater. Sci. Eng. R-Rep.* **2008**, 62, 37.

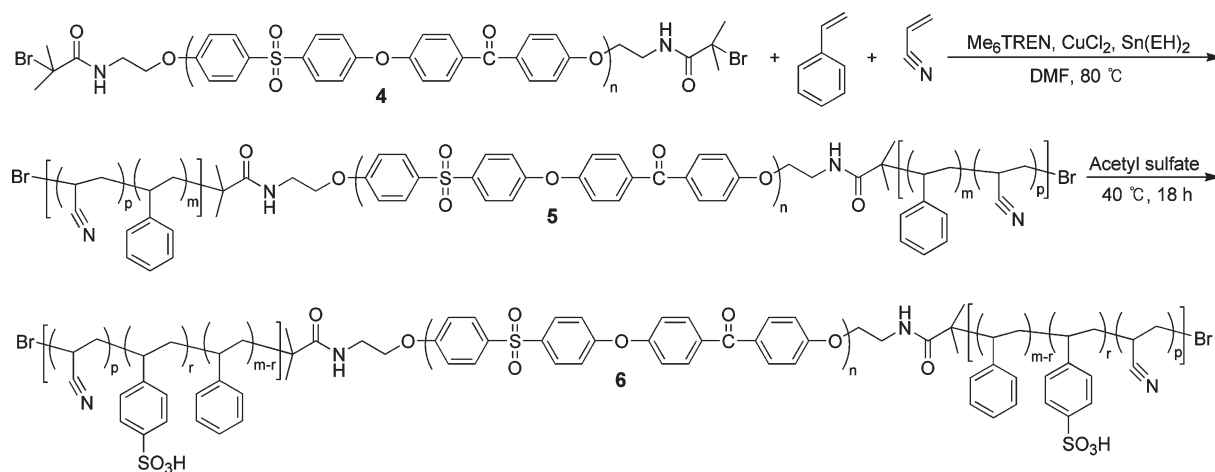
Scheme 2. Synthetic Scheme of PSEK-*b*-PSAN and Sulfonation

Table 1. Molecular Weights of PSEK (1) and Block Copolymers (5)

sample	$M_n$ (kDa)	$M_{n,rod}$ (kDa)	$M_{n,coil}$ (kDa)	PDI
1	18	18	0	1.52
5(18/12)	30	18	12	1.63
5(18/27)	45	18	27	1.73
5(18/42)	59	18	42	1.86

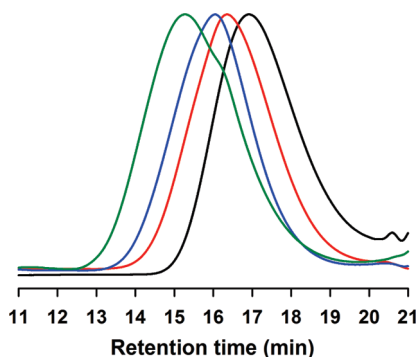


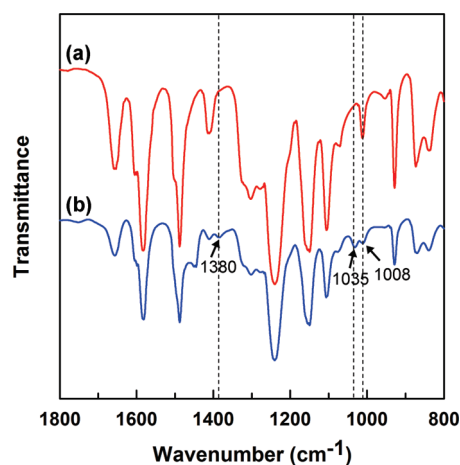
Figure 2. GPC traces of PSEK macroinitiator (black), 5(18/12) (red), 5(18/27) (blue), and 5(18/42) (green).

Table 2. Properties of Sulfonated PSEK-*b*-PSAN (6) Membranes

sample	degree of sulfonation <sup>a</sup> (%)	water uptake (%)	calculated IEC <sup>a</sup> (mmol/g)	measured IEC <sup>b</sup> (mmol/g)
6(18/12-3)	2.5	4.8	0.12	0.11
6(18/12-4)	4.2	6.0	0.22	0.21
6(18/12-7)	7.2	8.5	0.39	0.37
6(18/27-3)	2.7	3.1	0.14	0.12
6(18/27-6)	6.5	5.8	0.32	0.30
6(18/27-9)	9.3	8.0	0.46	0.45
6(18/42-2)	1.9	5.5	0.08	0.08
6(18/42-6)	5.5	7.6	0.26	0.25
6(18/42-9)	9.1	9.1	0.45	0.43

<sup>a</sup> Determined by elemental analysis. <sup>b</sup> Determined by titration.

was measured as a function of temperature at 100% RH (see Supporting Information, Figure S2), it revealed that the membrane made from 6(18/42-9) showing lamellar morphology exhibits the highest proton conductivity over the entire temperature range examined, whereas the

Figure 3. FT-IR spectra of (a) PSEK-*b*-PSAN and (b) sulfonated PSEK-*b*-PSAN.

membrane of 6(18/12-7) showing cylinder morphology exhibits the lowest proton conductivity. Figure 6 shows a more direct evidence for the effect of the internal structure on proton conductivity. When the normalized proton conductivity ( $\sigma/\phi$ ), as defined as the ratio of proton conductivity ( $\sigma$ ) to the volume fraction of hydrophilic domain ( $\phi$ ), is plotted against the degree of sulfonation, it is realized that the value of  $\sigma/\phi$  at the same degree of sulfonation increases as the morphology changes from HEX, HPL to LAM phase. It has been reported that the normalized proton conductivity per volume fraction of swollen hydrophilic domains in sulfonated polystyrene/poly(methyl methacrylate) block copolymer (coil-coil diblock copolymer) increases as the morphology changes from the disordered state HEX, HPL to LAM phase.<sup>33</sup> Therefore, our results are in good agreement with the previous report in terms of correlation between morphology and conductivity. It is also observed that the proton conductivity of all the membranes increases with increasing the temperature from 30 to 120 °C, as can be clearly seen in Figure S2.

(33) Rubatat, L.; Li, C. X.; Dietsch, H.; Nykanen, A.; Ruokolainen, J.; Mezzenga, R. *Macromolecules* **2008**, *41*, 8130.

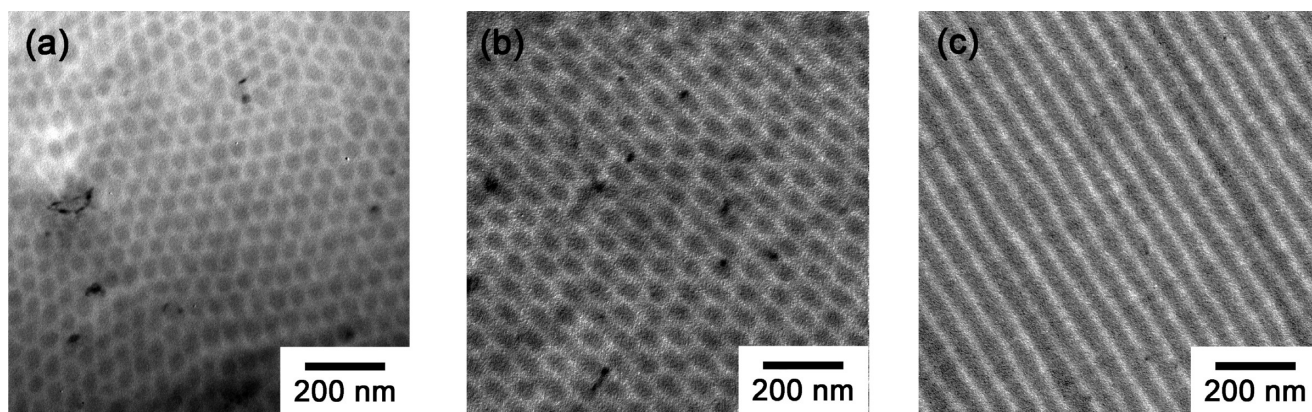


**Figure 4.** TEM images of (a) **6(18/12-7)**, (b) **6(18/27-9)**, and (c) **6(18/42-9)**. Dark and bright areas correspond to hydrophilic and hydrophobic phases, respectively.

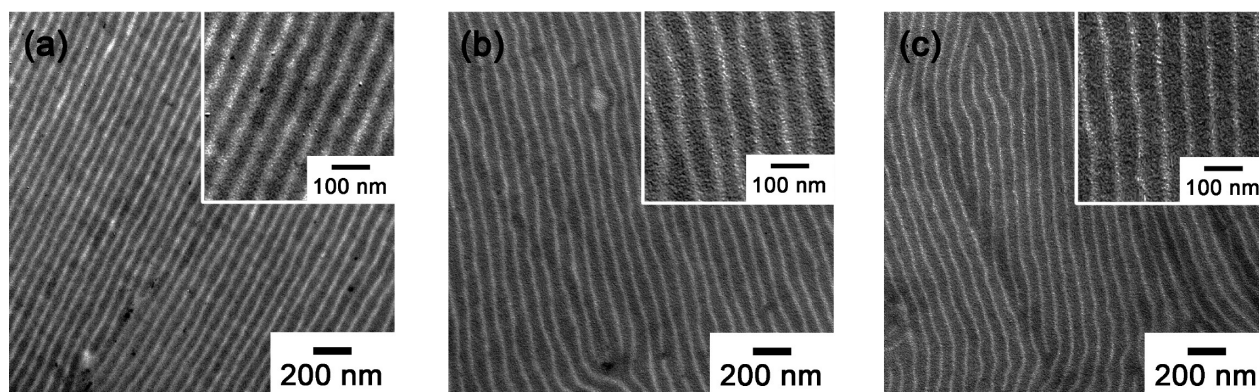


**Figure 5.** TEM images of (a) **6(18/42-2)**, (b) **6(18/42-6)**, and (c) **6(18/42-9)**.

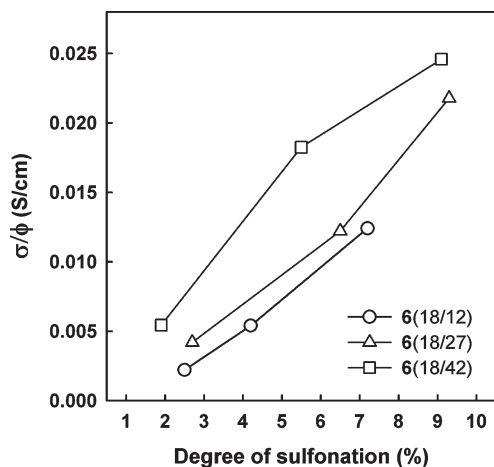


**Figure 6.** Normalized proton conductivity of membranes with different hydrophilic block length as a function of the degree of sulfonation (120 °C, 100% relative humidity).

When the proton conductivity is plotted against the hydration number ( $\lambda$ , the number of water molecules absorbed per sulfonic acid group), as shown in Figure 7, it is obvious that the proton conductivity of all membranes increases with the hydration number. More importantly, the proton conductivity of membranes at the same hydration number increases in the order of **6(18/12)** (HEX), **6(18/27)** (HPL), and **6(18/45)** (LAM), indicating

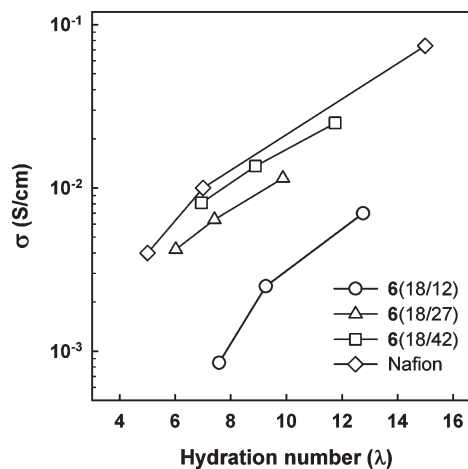


**Figure 7.** Dependence of proton conductivity of membranes at 120 °C upon the hydration number.

that the proton conductivity is strongly dependent upon phase-separated morphology and proton path connectivity. It is noteworthy here that the performance of **6(18/45)** (LAM) is comparable to that of Nafion, which suggests the formation of well-connected hydrophilic channel as good as that of Nafion.

When the conductivities of the membranes with different DSs are plotted against temperature in Figure 8, it is observed that the proton conductivity increases with

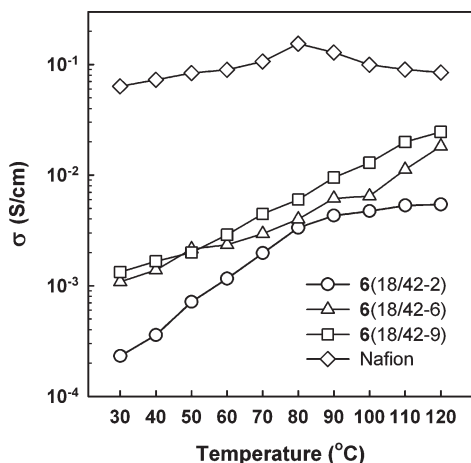


**Figure 8.** Proton conductivity of membranes with different DSs as a function of temperature at 100% relative humidity.

increasing the DS over entire temperature range examined. This is easily expected because higher sulfonation level results in higher number of proton charge carrier. Although the activation energy for proton transport through the membrane **6**(18/42-9), as calculated from the slope of  $\ln \sigma$  versus  $(1/T)$ , is about 37 kJ/mol, which is higher than that of Nafion, this value is almost the same as the activation energy of sulfonated PEEK with much higher ion exchange capacity (IEC) (1.2 mmol/g) and larger water uptake than ours (0.45 mmol/g),<sup>34</sup> indicating that our membrane has well-connected hydrophilic domains.<sup>35</sup> The activation energy of our membranes decreases with increasing the DS, but the energy difference among the samples with different DSs is not large (4–7 kJ/mol). It is also noted that the proton conductivity shows a tendency to increase with increasing temperature, irrespective of the sulfonation level.

**Thermal and Oxidative Stability.** The thermal stability of the block copolymers, as examined by thermogravimetric analysis (TGA), shows that the weight loss starts to occur above 170 °C (see Supporting Information, Figure S3), indicating that the block copolymers exhibit good thermal stability that is comparable to the thermal stability of membranes used in high-temperature fuel cells.<sup>6</sup>

Another important property for the long-term use of PEMs is oxidative stability. When the weight loss of the block copolymer membranes was measured as a function of time in Fenton's reagent at 80 °C as an accelerated test, all membranes exhibited much better stability to oxidation as compared with those of other polystyrene-based PEMs in the literature.<sup>36</sup> It should be mentioned that the oxidative stability is decreased as the volume fraction of the hydrophilic block is increased, indicating that the sulfonated PSAN block has lower oxidative resistance than PSEK block.

## Conclusions

In this study, novel amphiphilic rod–coil block copolymers composed of thermally and chemically stable PSEK

and sulfonated PSAN were successfully synthesized for application to fuel cell membrane. The membranes were observed to have different morphologies, hexagonally arranged cylinders, hexagonally perforated lamellae, and lamella, depending upon the hydrophilic block length in the copolymer. The membrane with lamellar morphology showed the highest proton conductivity over the entire temperature range examined. The proton conductivity of our membranes increases continuously as the temperature is increased up to 120 °C. Particularly, the proton conductivity of the membrane with LAM morphology is comparable to that of Nafion at low hydration numbers. The membranes also exhibited good thermal and chemical stability.

## Experimental Section

**Materials.** DFDPS (99%, TCI) was purified by recrystallization from toluene, and DHBP (98%, TCI) was recrystallized from ethanol. Potassium carbonate ( $K_2CO_3$ ) (99%, Acros) was dried overnight in a vacuum oven at 120 °C prior to use. Tris(2-dimethylaminoethyl)amine ( $Me_6TREN$ ) was prepared according to the method reported in the literature.<sup>37</sup> Sulfolane (99%) and methylene chloride (99.5%, Daejung Chemicals & Metals) were distilled from sodium hydroxide (NaOH) and calcium hydride ( $CaH_2$ ), respectively, prior to use. To remove the inhibitor, St (99%) and AN (99%) were passed through a column filled with neutral alumina and dried by distillation over  $CaH_2$ . All other reagents were purchased from Sigma-Aldrich and used as received.

**Synthesis of Hydroxyl Terminated PSEK (1).** PSEK was first synthesized by the nucleophilic substitution reaction of DFDPS with DHBP according to the method described in a previous report.<sup>38</sup> A 100-ml, three-neck flask equipped with a mechanical stirrer, condenser, and argon inlet adapter was charged with DFDPS (5.09 g, 20.0 mmol), DHBP (4.28 g, 20.0 mmol), and sulfolane (30 mL). After 20 min of stirring at 40 °C, anhydrous  $K_2CO_3$  (2.90 g, 21.0 mmol) was added to the reaction mixture. The mixture was stirred at 160 °C for 3 h and then at 220 °C for 4 h. Subsequently, the temperature of the reaction mixture was reduced to 100 °C, and DHBP (0.250 g, 1.17 mmol) and  $K_2CO_3$  (0.168 g, 1.22 mmol) were added to the reaction flask to ensure hydroxyl end group. The reaction mixture was further heated at 220 °C for 2 h and then cooled to room temperature. The viscous solution was dissolved in 300 mL of chloroform and then filtered. The filtrate solution was poured into 1000 mL of methanol. The precipitated polymer was filtered and dried under vacuum at 120 °C for 24 h.  $^1H$  NMR (300 MHz,  $CDCl_3$ ):  $\delta$  (ppm), 7.96 (m, 4H), 7.93 (m, 4H), 7.86 (m, 4H), 7.83 (m, 4H).

**Boc-Protected Amine Terminated PSEK (2).** A round-bottom flask equipped with a dropping funnel was charged with **1** (7 g, 0.250 mmol),  $K_2CO_3$  (0.346 g, 2.50 mmol), and 60 mL of dimethylformamide (DMF). After stirring at 90 °C for 1 h, 2-(boc-amino)ethyl bromide dissolved in 10 mL of DMF was added to the reaction flask through the dropping funnel over a period of 30 min. The reaction mixture was stirred at 90 °C for 48 h. The polymer solution was cooled to room temperature and precipitated in 800 mL of methanol. The product was collected by filtration, washed with methanol and water, and then dried

(34) Shi, Z. Q.; Holdcroft, S. *Macromolecules* **2005**, *38*, 4193.

(35) Li, Y.; Roy, A.; Badami, A. S.; Hill, M.; Yang, J.; Dunn, S.; McGrath, J. E. *J. Power Sources* **2007**, *172*, 30.

(36) Hubner, G.; Roduner, E. *J. Mater. Chem.* **1999**, *9*, 409.

(37) Inceoglu, S.; Olugebefola, S. C.; Acar, M. H.; Mayes, A. M. *Des. Monomers Polym.* **2004**, *7*, 181.

(38) Han, Y. K.; Chi, S. D.; Kim, Y. H.; Park, B. K.; Jin, J. I. *Macromolecules* **1995**, *28*, 916.

under vacuum at 120 °C for 24 h.  $^1\text{H}$  NMR (300 MHz,  $\text{CDCl}_3$ ):  $\delta$  (ppm), 7.96 (m, 4H), 7.93 (m, 4H), 7.86 (m, 4H), 7.83 (m, 4H), 4.11 (m, 2H), 3.54 (m, 2H), 1.45 (s, 9H).

**Boc Deprotection.** After **2** (6.56 g, 0.234 mmol) was dissolved in 100 mL of anhydrous methylene chloride under Ar, the solution temperature was maintained at 40 °C. Trifluoroacetic acid was slowly added to the reaction mixture, and the resulting mixture was stirred for 5 h. The reaction mixture was cooled to 0 °C and concentrated under vacuum. The crude product, amine terminated PSEK (**3**), was dissolved in 100 mL of methylene chloride and precipitated in methanol.  $^1\text{H}$  NMR (300 MHz,  $\text{CDCl}_3$ ):  $\delta$  (ppm), 7.96 (m, 4H), 7.93 (m, 4H), 7.86 (m, 4H), 7.83 (m, 4H), 4.11 (m, 2H), 3.54 (m, 2H).

**Synthesis of PSEK Macroinitiator (4).** After **3** (4.50 g, 0.161 mmol) was dissolved in 120 mL of methylene chloride at 40 °C for 30 min, triethylamine (4.47 mL, 32.1 mmol) was added to the solution. This reaction mixture was then stirred for 1 h; thereafter,  $\alpha$ -bromoisobutyl bromide was added dropwise. The reaction mixture was stirred for 72 h at 40 °C. The resulting product (PSEK macroinitiator) was precipitated in methanol and dried under vacuum at 120 °C.  $^1\text{H}$  NMR (300 MHz,  $\text{CDCl}_3$ ):  $\delta$  (ppm), 7.96 (m, 4H), 7.93 (m, 4H), 7.86 (m, 4H), 7.83 (m, 4H), 4.11 (m, 2H), 3.70 (m, 2H), 1.98 (s, 6H).

**ARGET ATRP of St and AN Using PSEK Macroinitiator.** ARGET ATRP of St and AN was carried out by modification of a procedure reported in the literature.<sup>26</sup> After **4** (0.500 g, 0.0179 mmol) was dissolved in 20 mL of DMF in a 50-mL pear-shaped flask, the polymer solution was degassed by three freeze–pump–thaw cycles. St (6.14 mL, 53.6 mmol), AN (2.29 mL, 34.8 mmol),  $\text{CuCl}_2$  (0.216 mg, 1.61  $\mu\text{mol}$ ), and  $\text{Me}_6\text{TREN}$  (13.4  $\mu\text{L}$ , 48.3  $\mu\text{mol}$ ) were transferred to a dry Schlenk flask. The resulting mixture was degassed by four freeze–pump–thaw cycles, and  $\text{Sn}(\text{EH})_2$  (10.4  $\mu\text{L}$ , 32.2  $\mu\text{mol}$ ) was then added to the mixture. The macroinitiator solution was added to the Schlenk flask, and the reaction vessel was placed in a thermostatted oil bath at 80 °C. The degree of polymerization was controlled by the polymerization time. Polymerization was stopped by opening the flask and exposing the catalyst to air. The resulting product (**5**) was isolated by precipitation in methanol.  $^1\text{H}$  NMR (300 MHz,  $\text{CDCl}_3$ ):  $\delta$  (ppm), 7.96 (m, 4H), 7.93 (m, 4H), 7.86 (m, 4H), 7.83 (m, 4H), 7.02–6.41 (m, 5H), 2.60 (m, 1H), 2.18–1.28 (m, 5H).

**Sulfonation of 5.** A 1 M solution of acetyl sulfate was prepared before sulfonation reaction. First, acetic anhydride (0.950 mL, 10.0 mmol) was dissolved in 5 mL of methylene chloride in a 25-mL flask. When sulfuric acid (0.350 mL, 6.57 mmol) was added dropwise to the solution at 3–5 °C, a transparent colorless solution was obtained. Then, 400 mg of **5** was dissolved in 15 mL of methylene chloride. The solution was stirred and refluxed at 40 °C, while a specified amount of acetyl sulfate solution was added slowly to the solution. After 18 h, the reaction was terminated by the addition of methanol, and the solvent was removed under reduced pressure. The residual polymer was washed repeatedly with distilled water and methanol until its pH became neutral. The sulfonated PSEK-*b*-PSAN (**6**) was then dried under vacuum for 24 h at 30 °C.

**Membrane Preparation.** The block copolymer (**6**) of 400 mg was dissolved in 6 mL of DMF and the solution was filtered through 0.45- $\mu\text{m}$  PTFE filters. The solution was cast onto a clean, flat glass dish. The dish was placed inside a covered container and dried at 70 °C for 2 days; thereafter, the dish was dried in vacuum at 90 °C for 1 day to ensure complete removal of DMF.

Tough and free-standing membranes with a thickness of 70–120  $\mu\text{m}$  were obtained.

**Characterization.** The chemical structures of the materials used in this study were identified by  $^1\text{H}$  NMR (Avance 300 and Avance 500, Bruker). Molecular weight and its polydispersity were measured by GPC (Waters) with a refractive index detector (Waters 2414) at a flow rate of 1 mL/min. Tetrahydrofuran was used as an eluent, and the molecular weights of the materials were calibrated by polystyrene standards. Infrared spectra were recorded on an IR spectrometer (FT/IR-660 plus, Jasco). Elemental analysis was performed with EA1112 (CE instruments). For observation of membrane morphology, the membrane was sectioned to yield 70-nm thick using a Leica microtome Ultracut UCT and placed on copper grids. TEM observations were performed on a JEOL JEM1010 at an accelerating voltage of 80 kV.

**Water Uptake, Ion Exchange Capacity, and Proton Conductivity.** Water uptake was determined according to the standard method. First, the mass of the dry membrane ( $W_{\text{dry}}$ ) was determined, after the membrane was completely dried in vacuum at 30 °C overnight. Then, the membrane was equilibrated in distilled water for 2 days at room temperature, and thereafter the membrane was weighed under a wet condition. The water uptake was calculated as the following equation: water uptake (%) =  $(W_{\text{wet}} - W_{\text{dry}})/W_{\text{dry}} \times 100$ , where  $W_{\text{wet}}$  is the weight of the hydrated membrane.

The IEC of the membranes was measured by elemental analysis and titration. The membranes were equilibrated in 2.0 M NaCl solution for 2 days; thereafter, the solution was titrated with 0.025 M NaOH solution using phenolphthalein as an indicator. After titration, the membranes were washed with distilled water and dried for 2 days at 30 °C under vacuum. The IEC was calculated according to the equation:  $\text{IEC} = V_{\text{NaOH}} \times M_{\text{NaOH}}/W_{\text{dry}}$ , where  $W_{\text{dry}}$  is the dry weight of the sample, and  $V_{\text{NaOH}}$  and  $M_{\text{NaOH}}$  are the volume (mL) and molar concentration of the NaOH solution, respectively.

The proton conductivity was measured by electrochemical impedance spectroscopy (VMP3, Biologic) using a Bekktech four-point conductivity cell. The cell temperature and humidity were controlled by a fuel cell test system (Smart II PEMFC test station, WonATech). The proton conductivity ( $\sigma$ ) was then calculated as  $\sigma = L/Rwd$ , where  $L$  is the distance between the electrodes (4.25 cm), and  $R$ ,  $w$ , and  $d$  are the impedance, width, and thickness of the membrane, respectively.

**Stability.** Thermal stability was measured by TGA. TGA were carried out with TA 2050 at a heating rate of 10 °C/min under a nitrogen atmosphere. For measurement of oxidative stability, small pieces of the membranes were soaked in Fenton's reagent (3%  $\text{H}_2\text{O}_2$  aqueous solution contacting 2 ppm  $\text{FeSO}_4$ ) at 80 °C as an accelerated test. The stability was evaluated by measuring the weight loss as a function of time.

**Acknowledgment.** We thank the Ministry of Education, Science and Technology (MEST), Korea for financial support through the Global Research Laboratory (GRL) program.

**Supporting Information Available:** FT-IR spectra of **1–4**, the plot of conductivity vs temperature, TGA traces of **6**(18/42) and sulfonated **6**(18/42), and the weight loss of membrane as a function of treatment time with Fenton's reagent. This material is available free of charge via the Internet at <http://pubs.acs.org>.